ANNALI DI GEOFISICA, VOL. XXXVI, N. 3-4, June-July 1993

Paleoseismology of great earthquakes of the late Holocene

Daniela Pantosti[1] **and Robert S. Yeats**[2]
[1] *Istituto Nazionale di Geofisica, Roma, Italia*
[2] *Oregon State University, Corvallis, OR, U.S.A.*

Abstract
The main goal of paleoseismology is the study of large earthquakes of the past on the basis of their geologic and geomorphic expression to provide new and useful information for seismic hazard evaluations. The recognition and dating of individual paleoearthquakes and/or of the cumulated deformation produced by repeated earthquakes on the same fault permit to characterize the seismic behavior of the fault itself. In fact, using traditional geologic and geomorphologic methodologies, paleoseismological investigations provide the insights to estimate the main parameters indicating the behavior of a seismogenic fault. These parameters, *i.e.* slip per event, slip rates, rupture extent, recurrence time, and elapsed time, form the geologic data base that is used to develop the segmentation and recurrence models as the basis of modern probabilistic analyses of seismic hazard. At present, paleoseismological data exist only for a limited number of seismic regions of the world but these investigations are already started, or are going to be started soon, in several other countries. In this report we briefly analyze the steps of the paleoseismological research, describing the more common techniques that are largely suitable for several regions of the globe, and that may provide good results for recognizing the expression of paleoearthquakes and quantifying the fault parameters.

1. Introduction

The importance of investigating the behavior of seismogenic structures for seismic hazard assessment led to the creation of the International Lithosphere Program Task Group II-3 on the study of the great earthquakes of the late Holocene. The group contains 30 members. Its main goal is to encourage the development of paleoseismology in all the countries where seismic risk is high and where it is essential to develop seismic hazard programs.

Paleoseismologic studies were started about two decades ago in the Western United States and in Japan mainly to extend the historical record of seismicity into prehistoric time. Since then paleoseismological investigations have begun in several additional countries highlighting the potential of geologic studies for the evaluation of seismic behavior of active faults and for the understanding of seismogenic processes in different tectonic environments (Matsuda, 1977; Sieh, 1978, 1984; Adams, 1980, 1989, 1990, 1992; Schwartz *et al.*, 1983; Deng *et al.*, 1984; Hall, 1984; Schwartz and Coppersmith, 1984; Sieh and Jahns, 1984; Talwani and Cox, 1985; Weldon and Sieh, 1985; Meghraoui *et al.*, 1988; Schwartz, 1988; Beanland and Berryman, 1989; Bell and Katzer, 1990; Sieh and Williams, 1990; Armijo *et al.*, 1991; Machette *et al.*, 1991; Niemi and Hall, 1992; Tsutsumi *et al.*, 1992; Fumal *et al.*, 1993; Pantosti *et al.*, 1993). In particular, paleoseismological study followed several main lines of investigation: 1) detailed mapping of fault scarps produced by (and geomorphic features displaced by) contemporary and recent large earthquakes and study of its geology and geomorphology; 2) trenching along the fault scarp; 3) study of strandline features uplifted or downdropped by earthquakes, and 4) study of deposits related to seismic shaking such as turbidites, landslides, rockfalls, plus study of tsunami deposits. Observations that can be obtained from these investigations provide information to estimate some of the main parameters that characterize a seismogenic fault: extent of the rupture and distribution of slip during an individual earthquake, time elapsed since the last large earthquake, recurrence intervals and variations in recurrence intervals and earthquake size, and slip rates. Starting from such geological data base developed for different seismogenic structures, Schwartz and Coppersmith (1984) proposed the hypothesis of the characteristic earthquake. This hypothesis states that individual fault segments tend to generate earthquakes of essentially the same size, displaying similar rupture length and coseismic slip. However, it has to be considered that in particular cases different rupture length have been observed (Berryman and Beanland, 1991; Weldon, 1991). A basic contribution for seismic hazard evaluations, directly derived from the Schwartz and Coppersmith hypothesis and from the geologic data base, is the development of segmentation and recurrence models. The segmentation models are based on the observation that fault zones do not rupture along their entire length during an earthquake, but they are segmented, and that the location of the rupture is not random but rupture boundaries are physically controlled. The segments can persist for several seismic cycles, and, therefore, their characterization can provide information on the seismic sources and on rupture initiation and termination (Schwartz and Coppersmith, 1984; Crone *et al.*, 1987; Berryman and Beanland, 1991; Crone and Haller, 1991; dePolo *et al.*, 1991; Zhang *et al.*, 1991). The earthquake recurrence models describe the rate or frequency of occurrence of earthquakes on a seismogenic structure or in a region. The recognition of the type of recurrence intervals that characterize a particular structure (characteristic, variable, and cluster) (Schwartz and Coppersmith, 1984; Schwartz, 1987, 1990), is critical to evaluate the hazard associated with the structure itself. Using these models, the seismic hazard can be quantified on the basis of modern probabilistic analyses that provide the probability of future earthquake occurrence on a particular fault segment during a period of time.

In this paper, we discuss the basis for developing paleoseismologic investigations, the methods that are commonly used in paleoseismology, and the different kind of results, their significance, and their limitations.

2. The paleoseismologic investigation

Paleoseismological investigations are based on the ability of geologists to recognize the geological expression of past earthquakes. These records are the direct consequence of the permanent deformation of the ground surface that large-magnitude earthquakes ($M \geq 6.5$) produce, reflecting the deformation at mainshock depth on the seismogenic fault. These deformations appear as fault scarps (fig. 1a and b), and as horizontal and vertical deformations detectable in a region of several km^2 around the seismogenic structure (fig. 2a and b).

The fault scarp can be seen as the continuation of the seismogenic fault plane toward the surface; as a consequence its characteristics are an expression of the main parameters of the fault plane that ruptured at depth. Recent earthquakes for which geologic, geodetic, and seismologic data were available clearly indicate that there is definitely a consistency with geologic observations that can provide the geometry of the rupture, a minimum length, a minimum slip, and the slip distribution. Indeed, on the basis of a fault scarp study, a realistic estimate of the size of the earthquake that produced the scarp may be possible; this is particularly important for those earthquakes that occurred prior to the instrumental era.

Regional deformation varies in terms of size and sign (uplift or subsidence) depending on the position of each individual point of the surface with respect to the seismogenic source, depending on the characteristics of the source itself (fig. 3a).

The paleoseismologic investigation is based

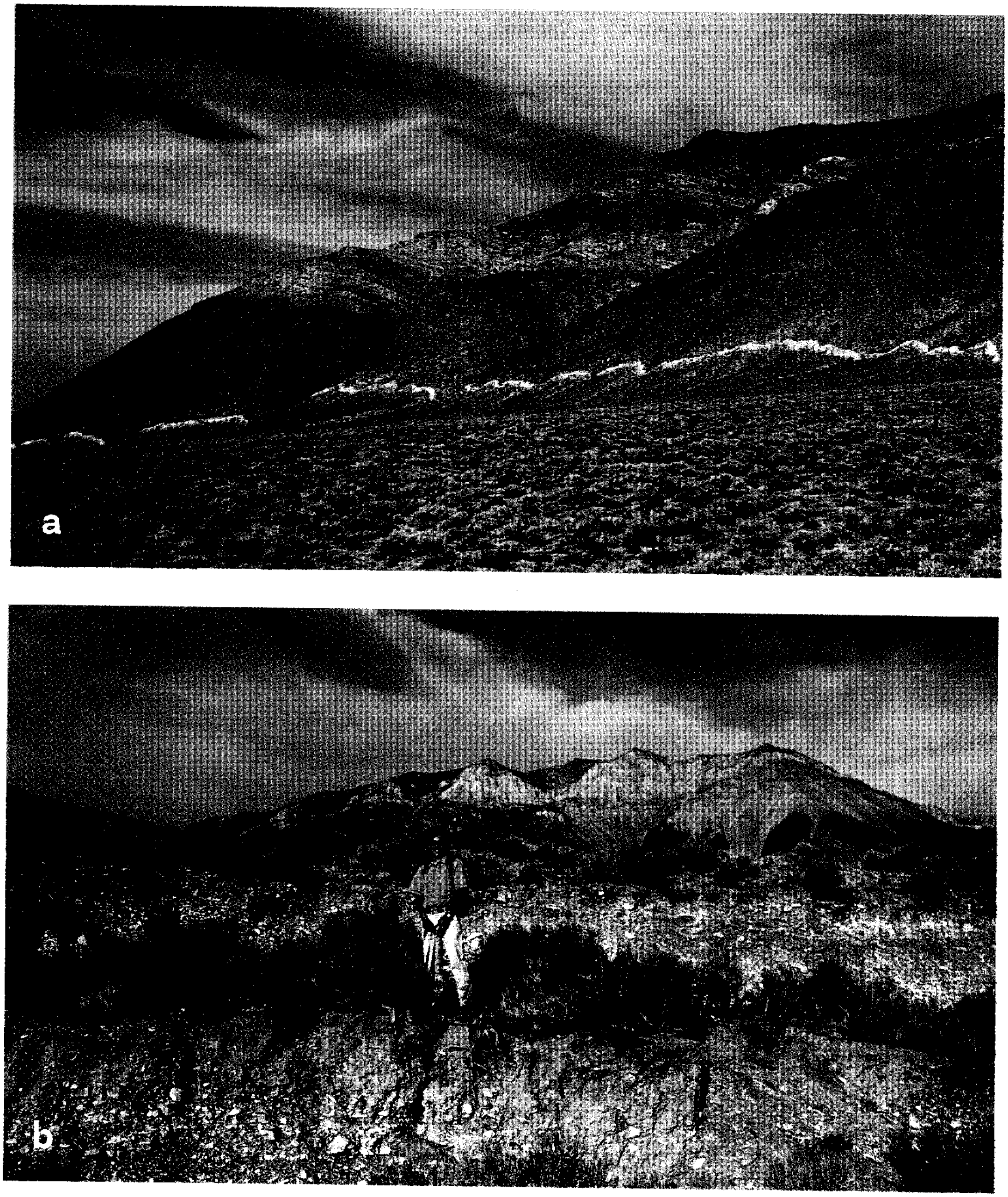

Fig. 1. a) View of the fault scarp produced by the 1915, Pleasant Valley (Nevada) normal faulting earthquake. The scarp runs at the base of the mountain range and bounds the adjacent elongated basin. Range and basin represent the long term effect of the tectonic activity of this fault (courtesy of G. Valensise). b) Detail of the 1983, Borah Peak earthquake fault scarp; at this site the fault scarp is formed by two ruptures very close to each other. Total vertical throw is about 3 meters.

2a

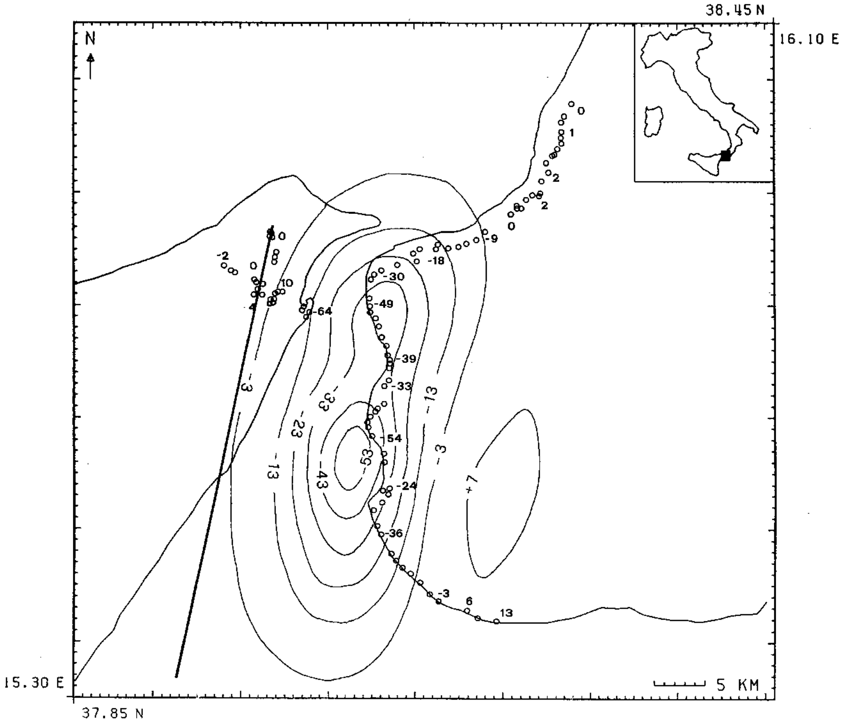
38.45 N
16.10 E
N
15.30 E
37.85 N
5 KM
-64
-49
-30
-18
-39
-33
-54
-24
-36
-53
-43
-33
-23
-13
-3
+7
13
6
-9
-2
10
0
1
2

b

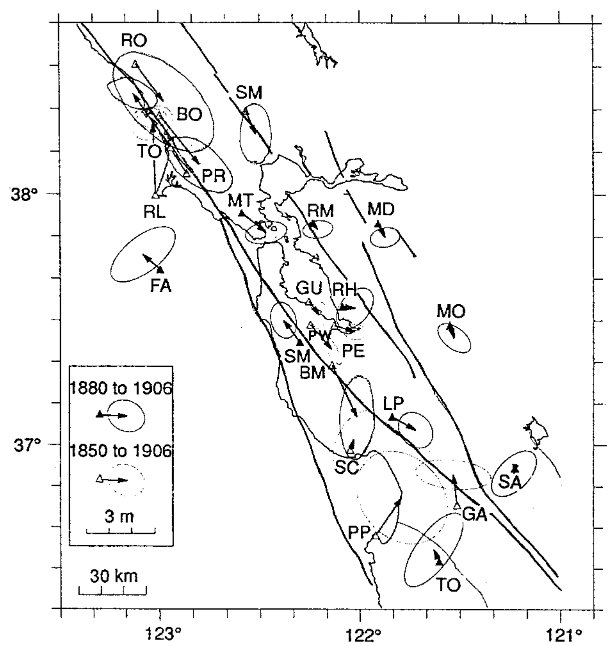
RO
BO
SM
TO
PR
RL
MT
RM
MD
FA
GU
RH
MO
PW
PE
SM
BM
LP
SC
SA
GA
PP
TO
1880 to 1906
1850 to 1906
3 m
30 km
38°
37°
123°
122°
121°

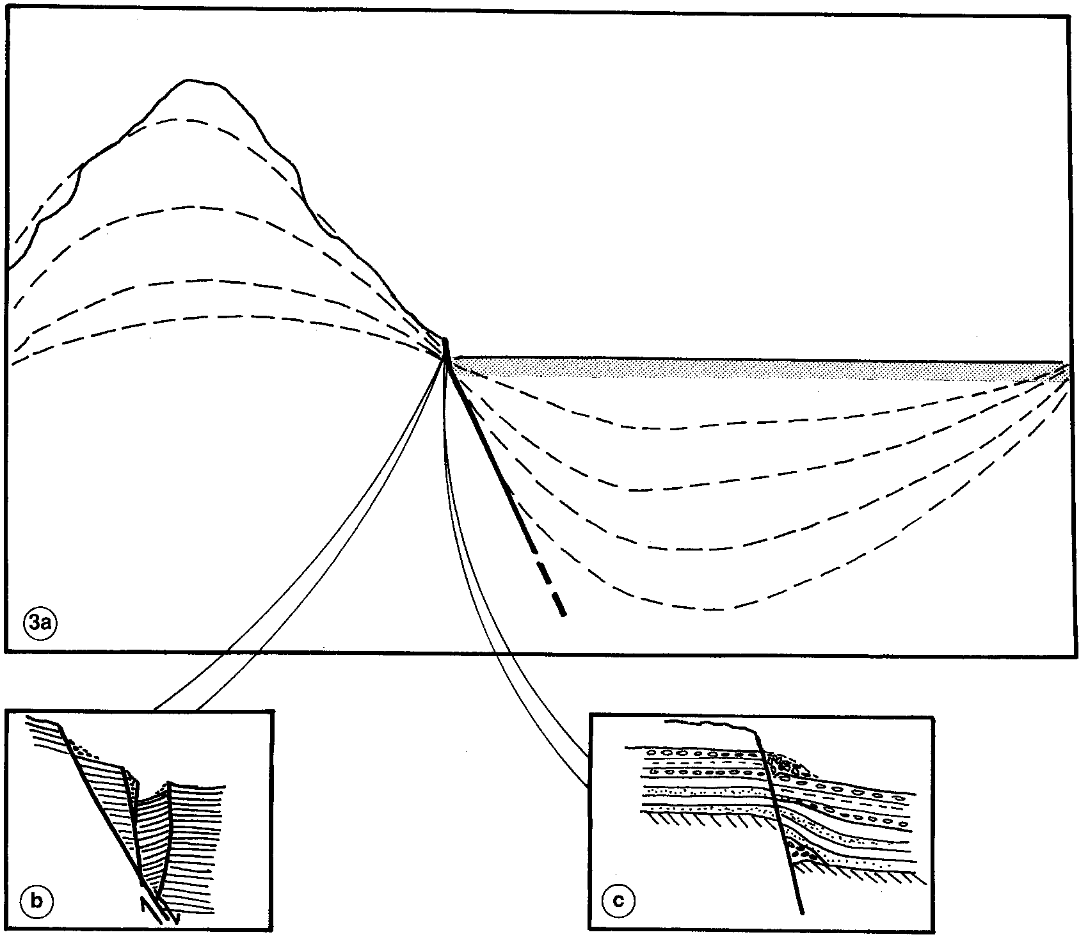

Fig. 3. a) Sketch showing the relationship between seismogenic normal faulting, the fault scarp, and the regional deformations. The dashed lines indicate the subsequent stages of growth of the structure that can be seen as individual coseismic changes. The base of the basin becomes deeper and sediments tend to fill it as soon as it subsides. b) and c) details of the near fault structures and sediments related to the disequilibrium created by the earthquake.

Fig. 2. a) Coseismic elevation changes produced by the 1908, Messina (Italy) earthquake; small circles are the benchmark locations (for some of them the coseismic change is indicated in cm). The thick line represents the projection to the surface of the seismogenic fault plane. The countours (in centimeters) represent the predicted elevation changes obtained by standard elastic dislocation modeling (Boschi *et al.*, 1989) and show clear coseismic subsidence in the Straits consistent with a E-dipping plane. Notice the extent of the region affected by coseismic elevation changes (redrawn from Boschi *et al.*, 1989). b) 1906 San Francisco earthquake horizontal displacements. The arrows show the size and versus of ground movement measured at the stations (triangles, the letters indicate the station name). The displacements reported in the figure are entirely consistent with the right lateral strike slip that occurred during the earthquake (from Segal and Lisowski, 1990).

on the observation that the permanent coseismic deformation of the surface creates a disequilibrium, both at local and regional scale, in the geomorphic processes that were occurring on the surface at the time of the earthquake. This disequilibrium is mainly due to the coseismic formation of relatively uplifted and subsided areas (fig. 3a, b, and c). As a result, new erosional and sedimentary processes take place trying to restore equilibrium. The erosional features and sediments that derive from these new processes become the geologic records of the past earthquakes that produced surface faulting. These records form and have a chance to be preserved in strict dependence on the geomorphic setting of the area (topography and type of rocks outcropping) and on the climatic conditions. Unfortunately, in many cases, successive re-erosion of the fault scarp itself and/or of the sediments and features providing evidence for the paleoearthquake may cause the partial or complete disappearance of the coseismic features.

However, when favorable geomorphic conditions permit, it is possible to recognize 1) the cumulated deformation of repeated earthquakes and/or 2) the occurrence of individual earthquakes.

There are no paleoseismologic standardized techniques to recognize unequivocally the evidence for past earthquakes. Each site and each structure require a different method of study. In the following, we discuss some examples of the most common techniques used in paleoseismologic investigations.

2.1. *The near-fault geomorphology*

The geomorphic study of a fault zone is the first and basic approach for recognizing

Fig. 4. The 1954 Hegben lake earthquake fault scarp still appears as a fresh cut of these alluvial deposits. Over this rupture it is possible to recognize a previous scarp whose height is of the same order of magnitude of the 1954 one and is clearly smoothed by erosional processes.

the evidence for past and repeated surface-faulting earthquakes that have occurred along that particular fault.

The fault-scarp morphology in soft sediments can be investigated to learn if a particular scarp is the result of one or more earthquakes.

In favorable geomorphic and climatic conditions, in fact, old fault scarps can be preserved if not buried (fig. 4).

Erosional processes take place, smoothing and degrading the scarp profile after its formation.

When a new scarp forms, it adds to the existing one, but its profile is bevelled (Wallace, 1977), but bevels disappear with time preserving a scarp too high for a single event. Several models correlating the evolution of the scarp profile to its age have been proposed (Nash 1980, 1986; Hanks *et al.*, 1984; Andrews and Hanks, 1985; Hanks and Wallace, 1985; Hanks and Schwartz, 1987). However, the high variability of the nature of faulted deposits and in different climatic conditions makes this modeling difficult and limits its application.

Information on past events can be obtained from the study of those geomorphic features that could be affected by slip along the fault. The most common and useful are streams, fans, alluvial terraces, basins, etc. These features, when influenced by tectonics, show anomalies and disturbances that can be used to detect individual earthquakes, but in general, they provide information for estimating the long-term deformation on the fault. The most common of these anomalies are deflected streams, rejuvenated stream profiles, abandoned, offset, or backtilted fans, diverted river beds, dammed basins, offset alluvial terraces, etc. (Sieh and Jahns, 1984; Mayer, 1986; Keller, 1986; Schumm, 1986; Lindvall *et al.*, 1989). For example the deflection of streams caused by slip along a strike slip fault can be accurately reconstructed and can provide individual (McGill and Sieh, 1991) (fig. 5a) or cumulated deformation along the fault (fig. 5b) (Sieh, 1981; Sieh and Jahns, 1984).

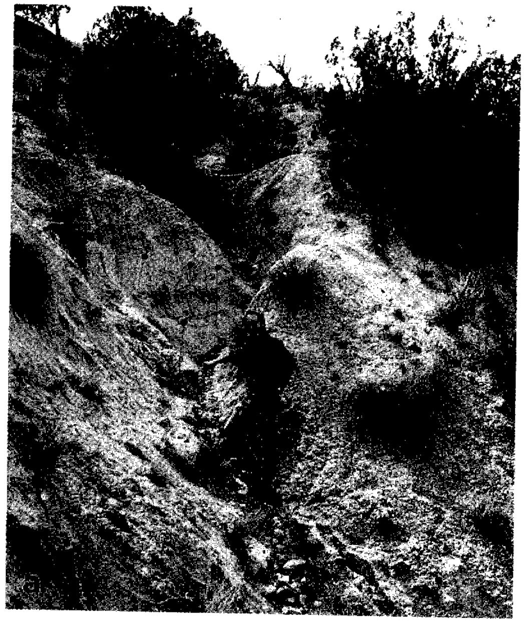

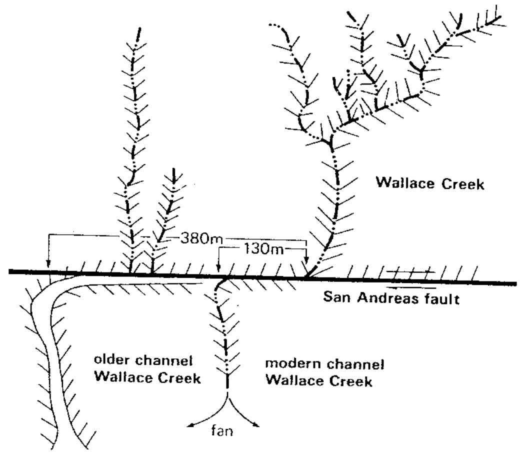

Fig. 5. Deflected streams along the San Andreas fault. a) 1857 earthquake stream-offset at Little Rock (Southern California). David Schwartz of the U.S. Geological Survey (in the photograph) put some colored reflectors (blue along the channel, red in correspondence of the fault trace) to highlight the offset that appears to be of about 3 m. b) Channel-offset at Wallace Creek along the San Andreas fault. The cumulated deformation shown by the older and modern channel of the creek is used to evaluate a long term slip rate (Late Pleistocene to Present) of 30 to 40 mm/yr (redrawn from Sieh, 1981).

2.2. *Regional geomorphology*

As mentioned above, coseismic deformation on the fault plane at depth affects a wide region of the surface and the amount of deformation at different sites is strictly dependent on the structure itself (geometry, type of movement, slip distribution). This deformation is also recorded geologically. The repetition of earthquakes along the same structure adds fault displacements and produces a distinct imprint on the geomorphology. This process can be seen in the origin of several regional features as ranges coupled with elongated basins (fig. 1a), linear valleys, overflooded and/or rejuvenated alluvial valleys, tilted paleosurfaces etc. A good possibility for quantifying the tectonic processes on a regional geomorphological basis is offered by some coastal environments. The coastal environment is very favorable because the sea level can be used as datum for relative and absolute elevation changes (Lajoie, 1986). The occurrence of individual earthquakes can be recorded as evidence of immediate subsidence or uplift of consistent parts of a coastline. The 1946 Nankaidos, 1964 Alaska, 1960 Chile, and 1991 Costa Rica earthquakes are good examples of these coseismic coastal deformations. However the non uniqueness of the cause producing coastal subsidence or uplift has to be considered, and independent observations to constrain the occurrence of the paleoearthquakes are needed. A good example of assembling different and independent observations to document the occurrence of an earthquake and demonstrate the synchroneity of its effects has been recently presented for an earthquake 1100 years ago in the Northwestern United States (Adams, 1992; Atwater, 1992; Atwater and

Fig. 6. 125 Kyr-old marine terrace (isotope substage 5e) on the Calabrian coast of the Messina Straits (the arrow indicates the inner edge). The terrace surface is deformed (it shows lower elevation toward south, right of the photograph) as result of repeated characteristic earthquakes. The terrace elevations, compared to the changes of elevation produced by the 1908 Messina earthquake were used from Valensise and Pantosti (1992) to infer the tectonic rates on the 1908 fault.

Moore, 1992; Bucknam *et al.*, 1992; Karlin and Abella, 1992; Jacoby *et al.*, 1992; Schuster *et al.*, 1992).

An extremely useful tool for estimating the velocity of tectonics as well as the geometry and distribution of the deformation is represented by marine terraces of Holocene and late Pleistocene. These marine platforms form only under particular conditions strictly related to the velocity of the coastal vertical movements in relation to eustatic changes. The terrace surface can be considered subhorizontal and gently dipping toward the sea at the time of its formation. In particular the terrace inner edge, representing the highest sea level reached during the terrace formation, if it is subjected to subsequent modification, can be considered as a line of long-term benchmarks formed at a relative zero level. If the terrace is located inside a region of influence of a seismogenic structure, each point of the inner edge records the changes in elevation produced at that particular site due to slip on the seismogenic fault. As earthquakes repeat along the same structure, deformation accumulates, and the terrace shows a direct imprint of the tectonic activity (fig. 6). Avoiding erosional and local effects, and considering sea level changes and interseismic adjustments, terrace inner edge elevations in some cases can be used 1) to define the seismogenetic structure using dislocation modeling; 2) to obtain long-term estimates of tectonic rates (Valensise and Ward, 1991; Valensise and Pantosti, 1992).

2.3 *Trenching*

Trenching of a fault scarp is probably the most common and high potential technique for

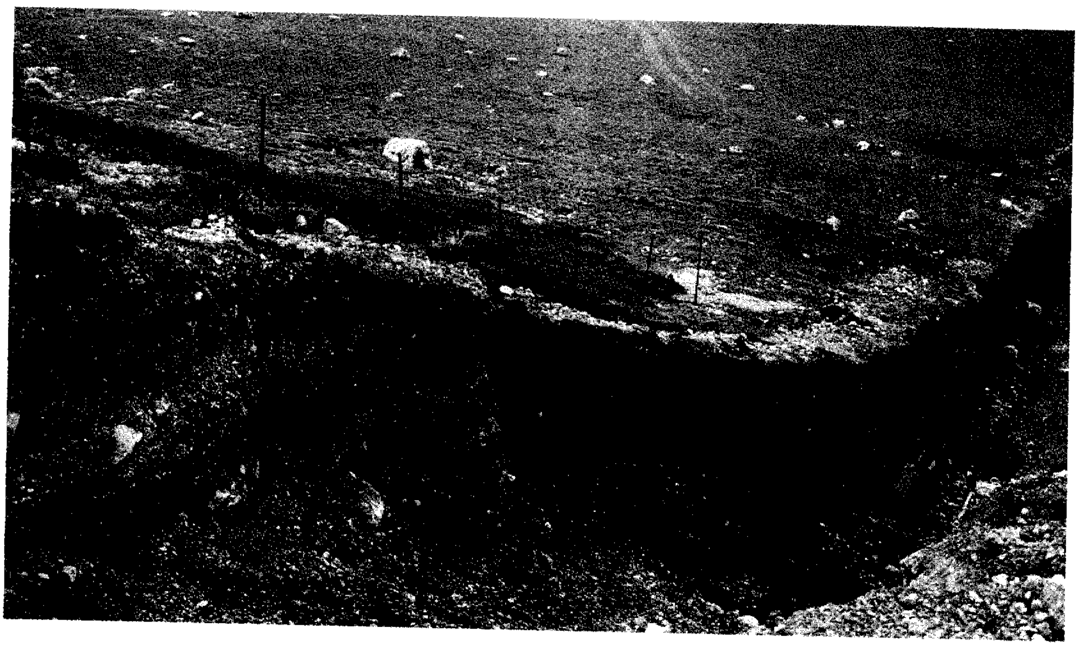

Fig. 7. Trench excavated across the normal fault of Piano di Pezza. For dip-slip faults it is sufficient to work in the two-dimensions exposed in the walls of the trench to investigate the slip along the fault. This trench is not shored; the cut is about 4-m wide. The main fault trace is shown by the red line. Notice the complex deformation of the deposits on the right of the fault. The dark layer indicated by the arrows is a soil that was faulted during the last earthquake that occurred along this fault. This soil is buried by an unfaulted colluvial wedge.

investigating an active fault with surface rupture. Because of the wide application of this type of investigation, we describe it in greater detail. The study is concentrated on the recognition of the geological evidence for past surface-faulting earthquakes. As discussed above, the evidence of past surface-faulting events does not have the same likelihood of preservation or recognition at every site along the fault. Therefore, the selection of the trench site should be done very carefully. Two conditions have to be satisfied: 1) the location of the fault scarp at the site should be known with uncertainty of no more than a few meters, and 2) the geomorphic setting of the site should favor sedimentation to make more likely the preservation by burial of the geologic records of past earthquakes. The trench location should be selected in order to maximize the preservation of datable sediments cut by the fault. It may be better to trench where alluvium is preserved on both sides of the fault, even if displacement per event is less, in order to get more events preserved on both sides of the fault at trenching depths. Depending on the type of fault under investigation, the trenches will be located in different ways. For mainly dip-slip faults, trenches are excavated perpendicular to the fault scarp (fig. 7), whereas strike-slip faults require the excavation of a double set of trenches, parallel to and perpendicular to the scarp (fig. 8). In the first case, slip along the fault, being essentially vertical, can be evaluated on the exposure of the fault zones. In the other, the reconstruction of piercing lines in fault-parallel trenches is necessary to evaluate horizontal slip. Trenches are generally excavated by a backhoe or a bulldozer. However, a few days of hand excavation can result in opening a

Fig. 8. Trench site on the Rodgers Creek strike slip fault (North San Francisco bay). The fault runs across this little alluvial basin (the main fault trace is indicated by arrows) and forms a little pressure ridge clearly cut by the two trenches on the left. Two sets of trenches have been opened, parallel and perpendicular to the fault, to investigate the slip along the fault by reconstructing piercing lines and recognize the occurrence of repeated faulting events as recorded in the fault zone. Trenches are about 1 m-wide and are shored by using hydraulic jacks set each 2 m.

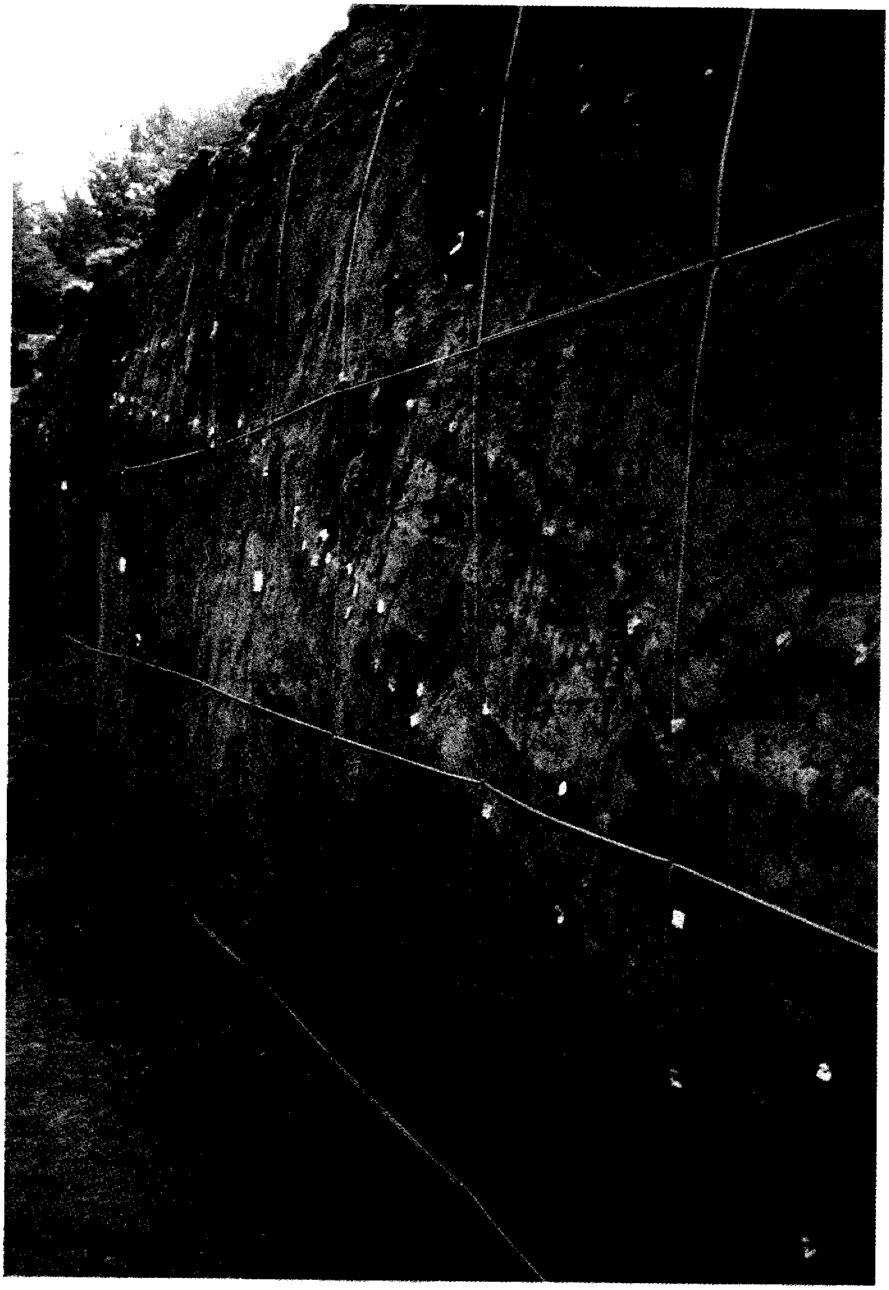

Fig. 9. Detail of a trench wall with flagging and reference net. In this trench across the Irpinia fault (Southern Italy) the fault zone appears as a warping of sediments and ground surface. Individual events have been recognized in this trench on the basis of stratigraphic indicators and increasing displacements from Pantosti *et al.* (1993). The discordancy existing between the layer flagged in pink and that in yellow is interpreted as one evidence of the occurrence of a paleoearthquake.

trench in those regions that are not reachable with these excavation machines or where hand labor is inexpensive, such as in China. In general, a trench is 20- to 30-m long, 3- to 4-m deep, and 1- to 4-m wide. In any case the trench should be extended far enough from the fault to reach sediments undisturbed by faulting. The relationship between width and depth of a trench, taking into account the kind of sediments excavated, is important for trench stability and safety of the people examining the trench walls. Trench walls can be shored to increase their stability; in these cases, the trench width can be as small as 1 m (fig. 8). Shoring can be executed by building a wooden frame, by using screw-jacks, or hydraulic jacks. If shoring is not possible the trench should be 3 to 4 m wide (fig. 7); safety can be increased by excavating a 1-m-wide, 1-m-deep step in one of the two walls. Once the trenches are open and possibly shored, smoothing of the trench walls is performed by hand using garden or construction tools. The wall is made as planar as possible, so that the sedimentary features and tectonic structures show clearly. Important features are highlighted by painted nails or little colored flags pierced by nails. A further step for the preparation of a trench for its study is the setting of a horizontal and vertical grid formed by 1 m-wide squares outlined by string or twine; these serve as a reference for logging trench walls and for correlating features to other trenches at the same site (fig. 9). Once the preparation phase is concluded the trench walls are logged generally at a scale of 1:20 (vertical and horizontal) to show in detail all the features and structures exposed (fig. 10). Along with the logging, the interpretation of the relationships between sediments and structures in the trench is performed. The possible geological records of individual paleoearthquakes are highlighted and, at the same time, the geometry, type of movement, and amount of deformation for each event evaluated. In some cases, it is possible to recognize only the evidence of cumulated deformation of repeated events. The stratigraphic level that was the ground surface at the time of a specific paleoearthquake is generally referred to as an event horizon. The final but critical step in the study of a trench is to date the event horizons to constrain the ages of the paleoearthquakes on the fault. In general, an age range for each event is constrained by the age of the sediments above and below each particular event horizon (see section 3).

The most common features that indicate the formation of a fault scarp are *colluvial wedges*. These are directly related to the sudden and sharp change in elevation of the ground surface that in general is caused by slip on a dip slip fault, or because of lateral juxtaposition of topography. Colluvial wedges are wedge shaped deposits that partially bury the scarp and are derived from erosion of the scarp itself (fig. 7, 10 and 11). The colluvial wedge represents indeed a post-earthquake deposit; the event horizon is located at its base. The wedge postdates the event, and the deposits that it buries predate the event. Figure 12 shows the formation of colluvial wedges and their subsequent faulting related to the occurrence of a more recent earthquake. The colluvial wedge is equivalent to the debris slope and wash slope of Wallace (1977).

Sometimes the coseismic deformation is accompained by a tilt of the sedimentary beds both because of near-fault complexity and because the fault scarp is accompained by a flexure of the ground and sediments, rather than a sharp rupture. When sedimentation starts again after the earthquake, an angular unconformity forms in the sequence, and the new sediments onlap the fault scarp (fig. 10 and 13). This unconformity represents an event horizon.

Event horizons can be also located on the basis of upward terminations of faults. The fault scarp is commonly characterized by a zone formed by several fault splays. The main fault traces are usually activated during repeated faulting events while the secondary splays may not slip during the subsequent events and may be buried beneath unfaulted sediments (fig. 10). The base of these unfaulted sediments, capping a fault splay, represents indeed an event horizon. However discussion is open about the possibility of having apparent upward terminations that are not evidence

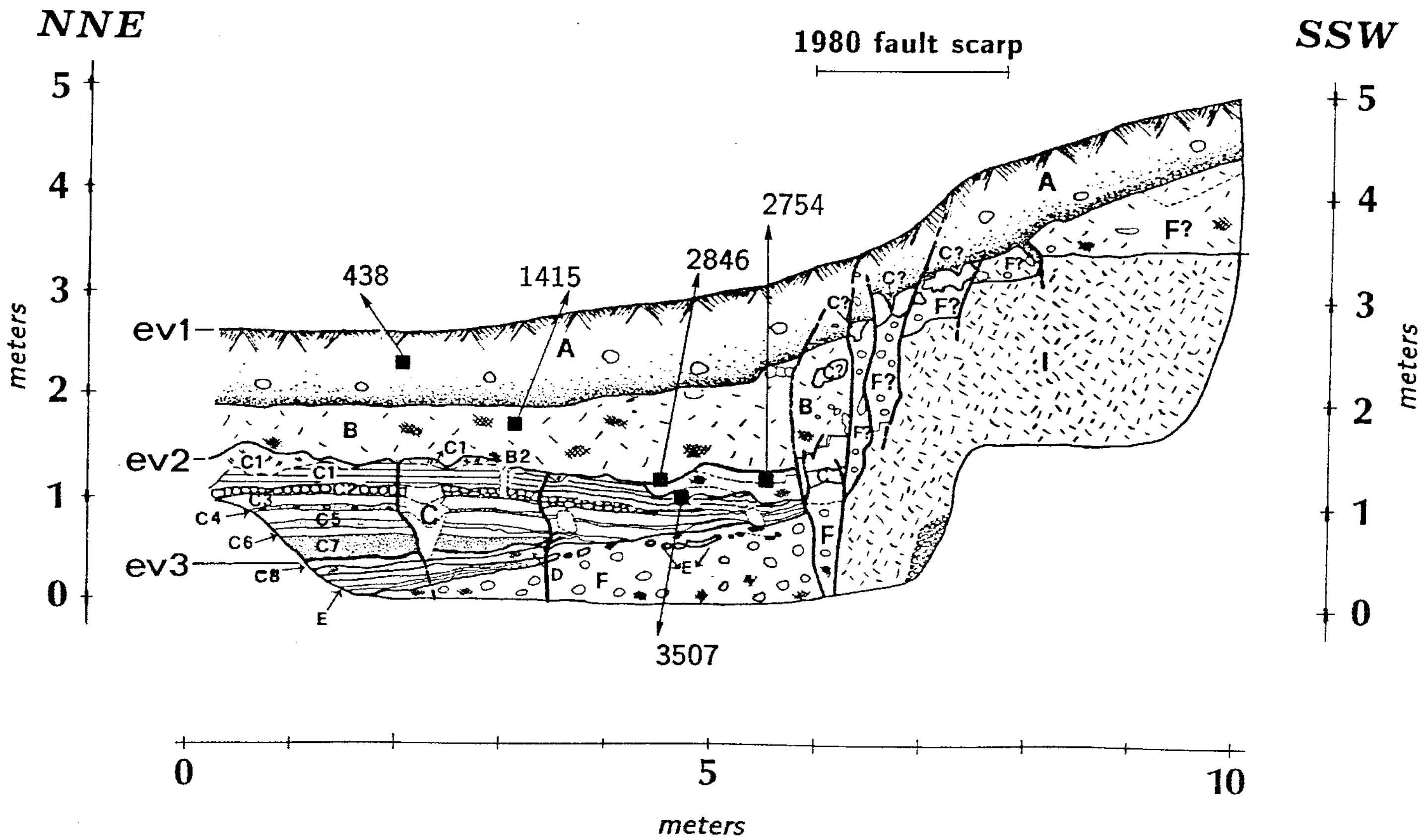

Fig. 10. Log of a trench opened across the 1980, Irpinia (Italy) earthquake surface rupture. The field log was made in detail at a 1:10 scale and then reduced for publication. The stratigraphic sequence is composed of lacustrine (C and E), colluvial and slope-wash (A, B, D, and F) deposits all faulted in correspondence to the 1980 rupture. Black squares locate the carbon samples for which radiocarbon dating was suitable; their calibrated age (calendar years B. P.) is indicated. Three event horizons have been recognized: **ev1** is the present ground surface and correspond to the 1980 earthquake; **ev2** is located at the base of the colluvial wedge B and in correspondence of the upward termination of the secondary fault located at m 2 that did not rupture during the last earthquake; **ev3** corresponds to the discordancy between C8 and C7 (see fig. 13). Age of the paleoearthquakes is constrained using the age of dated samples: **ev2** occurred sometime between 2754 and 1415 calendar years B.P.; **ev3** is older than 3507 calendar years B.P. (modified from Pantosti *et al.*, 1993).

Fig. 11. Trench excavated across the 1983, Borah Peak earthquake rupture. The main fault traces, forming a graben-structure, are indicated with the red lines. Degradation of the fault scarp started immediately after the earthquake and typical colluvial wedge deposits started accumulating at the base of the scarp itself. The 1983 colluvial wedge (lighter colored deposits) that buries part of the free-face (dotted line) is recognizable on the right side of the photograph. The trench walls show also a previous colluvial wedge (indicated by a star) that formed following a previous surface faulting earthquake and that was faulted in 1983 (courtesy of D.P. Schwartz).

for the occurrence of a faulting event at that particular level in the stratigraphy; this seems to be particularly likely for strike-slip faults (Bonilla and Lienkamper, 1990).

Further evidence for repeated surface-faulting earthquakes is the detection of increasing amount of deformation with increasing age of sediments. This can be particularly clear when there is a vertical component of slip. If the sediments are well bedded, the vertical displacement recorded by the sediments can be measured in detail. If in a sequence with the same amount of displacement, this is distinctly greater than that of an overlying sequence, the boundary between the sequences can be interpreted as an event horizon (fig. 13). When the stratigraphy is massive, and bedding can not be discriminated, it is possible to estimate only the long-term deformation accumulated along the fault during a certain interval of time. This is frequently the case of the offset recorded by piercing lines (*i.e.* stream channel, fan boundaries, terrace riser, etc.) across a strike-slip fault.

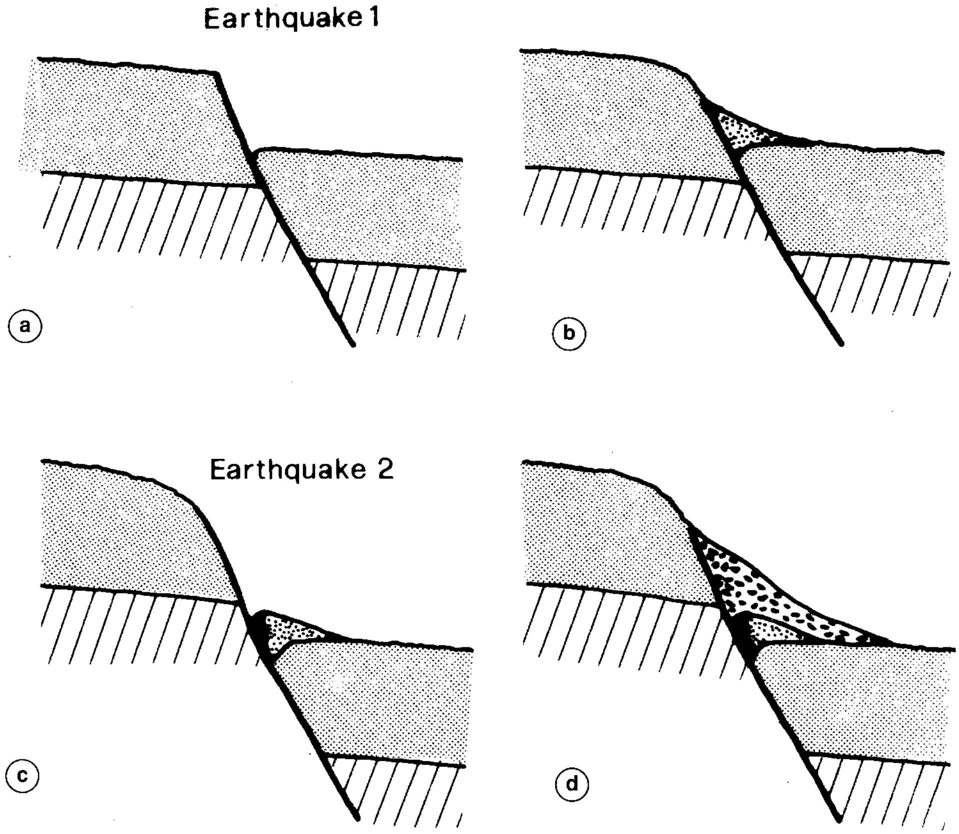

Fig. 12. Cartoon showing the near-fault relations between surface faulting, sedimentation, and erosion: a) a fault scarp abruptly forms on the ground during earthquake 1; b) a colluvial wedge forms at the base of the scarp that appears smoothed by the post-earthquake erosional and sedimentation processes; c) earthquake 2 produces a further displacement of the bedrock and the faulting of the colluvial wedge. The scarp at the surface represents the cumulated effect of the two earthquakes; d) a new colluvial wedge forms in response of the disequilibrium created at the surface by earthquake 2 (redrawn from Schwartz and Coppersmith, 1984).

2.4 *Stratigraphy*

Other effects of earthquakes can be recognized in stratigraphic sections as far as several hundred of kilometers from the seismogenic source. Their origin is related to the shaking produced by earthquakes and depends on particular site conditions. This is the case of liquefaction, slumping, slides, rock falls, turbidites, tsunami deposits, and so on. These earthquake effects can provide information on the accelerations reached at a certain site or on the arrival of a tsunami wave at a particular time but they do not provide information to characterize the seismogenic structure responsible for that event. Moreover as already mentioned for coastal environments, most of these effects can be produced by sources different from earthquakes such as storms, overloading of sediments, slope instability, etc.

Although there are many uncertainties, these observations, if accurately selected and

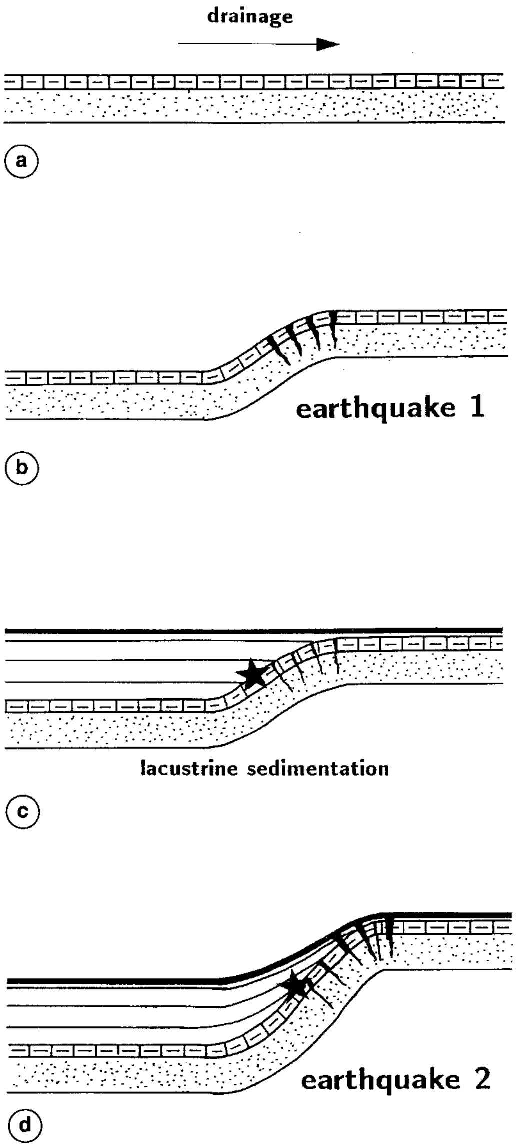

Fig. 13. Piano di Pecore basin faulting and filling process. When a fault scarp forms across the basin it forms a warping of the surface and sediments (b). The scarp interrupts the drainage and the post-earthquake sediments onlap the scarp showing a clear discordancy with the pre-events deposits in the fault zone (c). This discordancy (indicated with a star) corresponds to an event horizon. A successive earthquake produces a new fault scarp and the process starts again (d) (from Pantosti *et al.*, 1993).

constrained with other observations, represent a powerful investigation technique especially in those regions where the seismogenic structures are not clearly expressed at the surface, such as blind faults, and earthquakes are not energetic enough to produce detectable modification of the ground. As mentioned above regarding coastal environments, a good example of the recognition of stratigraphic evidence of past earthquakes comes from the Western United States. In the Eastern United States, liquefaction features (sand volcanoes, sand pipes, convoluted beds, etc.) have been studied, and on the basis of their synchroneity over a vast region, they provide evidence for timing of paleoearthquakes (Talwani and Cox, 1985).

3. Dating techniques and problems

A critical part of the paleoseismological investigation is the timing of paleoearthquakes and the dating of sediments or geomorphic features that record the deformation.

The most common method for dating in paleoseismology is the ^{14}C. Quaternary continental deposits may contain charcoal fragments, organic layers, and soils that may be used for ^{14}C dating. Conventional ^{14}C dating needs several grams of charcoal or a larger amount of enriched material that unfortunately are not always available. In recent years a great improvement for paleoseismological research came from the use of Acceleretor Mass Spectrometry (AMS) for ^{14}C dating. AMS dating although more expensive than conventional dating allows the use of only a few milligrams of carbon. The laboratory ^{14}C measurements are in general corrected on the basis of the ratio $^{12}C/^{13}C$, this ratio provides information on the possible contamination of the sample deriving from young materials. Finally because the atmospheric ratio of $^{14}C/^{12}C$ has not been constant through time, the laboratory radiocarbon age must be corrected to calendar years with the use of calibration curves derived from samples of wood of known age (Pearson *et al.*, 1986) (fig. 14). The calibration of the radiocarbon age, because of the great

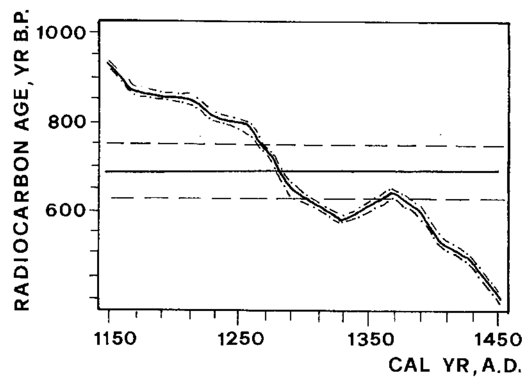

radiocarbon age: 690 ± 60 yr B.P.
calibrated age: 1312 ± 48 A.D.

calibrated age ranges:
– one sigma:
1262 - 1312 A.D. (66.2%)
1352 - 1385 A.D. (33.8%)
– two sigma:
1230 - 1398 A.D. (100%)

Fig. 14. Example of dendrochronological calibration for the radiocarbon measured age of 690 ± 60 years B.P. (Before Present, where present is the year 1950) to calendar years A.D. The curve is from Pearson *et al.* (1986) and the dashed-dotted lines represent the error on this curve. The dashed lines represent the error on the measure. In the lower part of the figure is given the calibrated age and the possible calendar age ranges calculated on the basis of the probability distribution for 1 and 2 sigma.

irregularity of the calibration curves, generally provides a complex probability distribution of the calendar age that gives a best calibrated age that is not very representative of the true age and several final possible calendar data ranges (fig. 14). Other uncertainties on the true age of the sample dated by using radiocarbon exist and have to be carefully considered. For example an anomalous initial ratio or subsequent changes of the ratio $^{12}C/^{14}C$ in the reservoir may have an important influence on the age we measure. In fact, the reservoir may be highly influenced by the presence of a carbonatic bedrock or by changes in the size of the body of water, in particular in case of lakes or during ice periods (Stuiver *et al.*, 1991). Also possible contamination of samples during burial, both with recent or old carbon, has to be considered. In particular contamination can produce unequal effects depending on the true age of sample, and on the type and amount of contamination (Grootes, 1983). Finally, in the case of dating shells, it is very delicate to distinguish the primary aragonite from that subsequently recrystallized. This would make the age much younger than the true one.

An important improvement to the estimate of the age of faulted surfaces is provided from the study of soil development and soil chemistry. Soil chronosequences have been compiled for several regions on the basis of chemistry, texture and thickness and, in some cases, constrained with some absolute dating (Harden, 1982; Harden and Taylor, 1983; Birkeland, 1985). For some regions, the degree of development of pedogenic calcium carbonate has been used as an indicator of soil development (Machette, 1985; McFadden and Tinsley, 1985).

One other promising method for dating faulted deposits is the thermoluminescence (TL) (Forman, 1989; Forman *et al.*, 1989, 1991). This method is based on the property of minerals like quartz and feldspar to be thermoluminescent for exposure at ionizing radiation (sunlight). TL age is measured in the laboratory by heating the sample to zero its thermoluminescence and rebuilding it starting from the time of burial of the minerals grains susceptible of dating.

On coastal deposits with faunas, amino-acid racemization and epimerization can provide important information on Quaternary chronology. However because racemization of a given species depends on temperature and a kinetic model, this method needs good calibration points that can be described by numerical methods (see for example Kennedy *et al.*, 1982; Lajoie, 1986 for the west coast of the United States).

Finally, tree-ring analysis can be used for dating paleoearthquakes. This method is based on the observation that trees living in the proximity of a seismogenic fault show disturbance in the growth of the rings forming at the time of occurrence of a large earthquake on that fault (Sheppard and Jacoby, 1989). It is clear that all other causes which could produce disturbances in the tree ring growth, such as drought, storms, flooding, have to be eliminated. The study starts from the sampling of non-destructive cores from a number of trees that are selected on the basis of age, size, topographic setting, and geologic setting, all indicators of the possibility of direct disturbances of the coseismic ground deformation on the tree growth. Cross-dating and careful checking are performed on several samples to document the disturbance, evidence of which should appear simultaneously in at least two trees. The applicability of this method is clearly limited by several factors such as age of trees with respect to the paleoearthquakes, proximity of trees to the fault, fault location etc. but is very promising for specific regions of the globe.

4. Paleoseismologic results

Geologic studies of historical and prehistorical earthquakes provide basic information on the behavior of seismogenic structures. Using different approaches (see previous paragraphs), the evaluation of cumulative slip in a certain amount of time and the timing and amount of deformation of individual earthquakes can be obtained for a particular fault. Starting from these geologic data, the main parameters that describe the seismic behavior of a fault that are commonly used for seismic hazard assessments are calculated. These parameters are all referred to the occurrence of repeated large earthquakes (M7) on a fault. We will briefly analyze these parameters, their meaning, and the basis for their calculation.

Slip per event is the amount of coseismic slip produced by one single event and is representative of the energy released during the earthquake. It can be evaluated only when individual events are recognized and is expressed as vertical and horizontal component of slip. If the dip of the fault plane is known, the slip on the plane can be calculated. During a single event, slip is not necessarily uniform along the fault; in most cases a high variability in slip is observed. Therefore an average value of slip, calculated on a large amount of observations along the fault, has to be considered.

Slip rate is the rate of deformation characteristic of a fault and is representative of the average activity of the fault and therefore of its strain-energy release. The slip rate is calculated on the basis of the deformation produced by the fault during a particular interval of time. Basic information are the age of the deformed sediments and the estimated amount of deformation. Depending on the observations that are available, slip rates can be calculated on the basis of short-term (Holocene) or long-term (late Pleistocene) deformation. Short-term evaluations are generally obtained from fault geomorphology and fault trenching whereas long-term slip rates are obtained from regional geomorphology (study of terraces, paleosurfaces, basin and range growth, etc.). Short-term evaluations are representative of the deformation during that particular period of time, while the long-term evaluations are based on the assumption that slip rate and displacement sense were constant during the longer interval of time.

Recurrence time is the average interval of time between two earthquakes on the same fault segment. When it is possible to recognize and date individual earthquakes on the fault, the average recurrence time can be directly calculated. Even without identifying individual earthquakes, an average recurrence time can be inferred from the slip rate and the slip per event, assuming that the slip per event is characteristic for the fault. In this case the average recurrence time can be seen as the time needed to accumulate enough deformation to be released during an earthquake producing the expected slip. Then, it can be calculated as slip per event divided by the slip rate. Individual recurrence intervals are also very important for the understanding of the fault behavior and are at the basis for recurrence models for main seismogenic structures. The time distribution of the earthquakes along single fault segments that form a seismogenic structure has been observed as essentially irregular. However characteristic of clustered recurrence times has been observed too. The definition of the type of recurrence time characterizing a structure is critical information for seismic hazard assessment.

Elapsed time is the time elapsed since the last earthquake occurred along that particular fault. It has a critical meaning in terms of hazard because if it is close to or larger than the average recurrence time it indicates that particular fault may have accumulated enough strain to release it seismically very soon. This is the basis for calculating the probability of the occurrence of an earthquake on a given fault.

REFERENCES

ADAMS, J. (1980): Paleoseismicity of the Alpine fault seismic gap, New Zealand, *Geology*, **8**, 257-262.

ADAMS, J. (1989): Postglacial faulting in Eastern Canada - Nature, origin, and seismic hazard implications, *Tectonophysics*, **163**, 323-331.

ADAMS, J. (1990): Paleoseismicity of the Cascadia subduction zone: evidence from turbidites off the Oregon-Washington margin, *Tectonics*, **9**, 569-583.

ADAMS, J. (1992): Paleoseismology: a search for ancient earthquakes in Puget Sound, *Science*, **259**, 1592-1593.

ANDREWS, D. J. and T. C. HANKS (1985): Scarp degraded by linear diffusion: inverse solution for age, *J. Geophys. Res.*, **90**, 10193-10208.

ARMIJO, R., H. LYON-CAEN and D. PAPANASTASIOU (1991): A possible normal-fault rupture for the 464 B.C. Sparta earthquake, *Nature*, **351**, 137-139.

ATWATER, B. F. (1992): Geologic evidence for earthquakes during the past 2000 years along the Copalis River, Southern coast Washington, *J. Geophys. Res.*, **97**, 1901-1919.

ATWATER, B. F. and A. L. MOORE (1992): A tsunami about 1000 years ago in Puget Sound, Washington, *Science*, **259**, 1614-1617.

BEANLAND, S. and K.R. BERRYMAN (1989): Style and episodicity of late Quaternary activity on the Pisa-Grandview fault zone, Central Otago, New Zeland, *N.Z. J. Geol. Geophys.*, **32**, 451-461.

BELL, J. W. and T. KATZER (1990): Timing of late Quaternary faulting in the 1954 Dixie Valley earthquake area, Central Nevada, *Geology*, **18**, 622-625.

BERRYMAN, K. and S. BEANLAND (1991): Variation in fault behaviour in different tectonic provinces of New Zeland, *J. Struct. Geol.*, **13**, 177-189.

BIRKELAND, P.W. (1985): Quaternary soils of the Western United States, in: *Soils and Quaternary Landscape Evolution*, edited by J. Boardman, J. Wiley, New York, pp. 303-324.

BONILLA, M.G. and J.J. LIENKAEMPER (1990): Visibility of fault strands in exploratory trenches and timing of rupture events, *Geology*, **18**, 153-156.

BOSCHI, E., D. PANTOSTI and G. VALENSISE (1989): Modello di sorgente per il terremoto di Messina del 1908 ed evoluzione recente dell'area dello Stretto, *Proceedings of VIII Convegno G.N.G.T.S.*, Roma, pp. 245-258.

BUCKNAM, R. C., E. HEMPHILL-HALEY and E. B. LEOPOLD (1992): Abrupt uplift within the past 1700 years at Southern Puget Sound, Washington, *Science*, **259**, 1611-1614.

CRONE, A. J., M. N. MACHETTE, M. G. BONILLA, J. J. LIENKAEMPER, K.L. PIERCE, W. E. SCOTT, and R.C. BUCKNAM (1987): Surface faulting accompaying the Borah Peak earthquake and segmentation of the Lost River fault, Central Idaho, *Bull. Seismol. Soc. Am.*, **77**, 739-770.

CRONE, A. J. and K.M. HALLER (1991): Segmentation and the coseismic behavior of Basin and Range normal faults: examples from East-Central Idaho and Southwestern Montana, U.S.A., *J. Struct. Geol.*, **13**, 151-164.

DENG, G. D., Y. WANG, Y. LIAO, W. ZHANG and M. LI (1984): Fault scarps, colluvial wedges on the frontal fault of M. Helanshen and its active history during Holocene, *Chin. Sci. Bull.*, **9**, 557-564 (in Chinese).

DEPOLO, C.M., D.C. CLAEK, D.B. SLEMMONS and A. R. RAMELLI (1991): Historical surface faulting in the Basin and Range province, Western North America: implications for fault segmentation, *J. Struct. Geol.*, **13**, 123-136.

FORMAN, S.L. (1989): Applications and limitations of thermoluminescence to date Quaternary sediments, *Quat. Intl.*, **1**, 47-59.

FORMAN, S.L., M.E. JACKSON, P. MAAT and M.N. MACHETTE (1989): An evaluation of thermoluminescence dating of paleoearthquakes on the American Fork segment, Wasatch fault zone, Utah, *J. Geophys. Res.*, **94**, 1622-1630.

FORMAN, S.L., A.R. NELSON and J.P. MCCALPIN (1991): Thermoluminescence dating of fault-scarp-derived colluvium: deciphering the timing of paleoearthquakes of the Weber segment of the Wasatch fault zone, North Central Utah, *J. Geophys. Res.*, **96**, 595-605.

FUMAL, T.E., S.K. PEZZOPANE, R.J. WELDON II and D.P. SCHWARTZ (1993): A 100-year average recurrence interval for the San Andreas fault at Wrightwood, California, *Science*, **259**, 199-203.

GROOTES, P.M. (1983): Radioactive isotopes in the Holocene, in *The Holocene*, edited by H.E. WRIGHT, (vol. 2 of late Quaternary environments of the United States), University of Minnesota Press., Minneapolis, pp. 86-105.

HALL, T.N. (1984): Holocene history of the San Andreas fault between Crystal Springs reservoir and San Andreas dam, San Mateo County, California, *Bull. Seismol. Soc. Am.*, **74**, 281-299.

HANKS, T.C., R.C. BUCKNAM, K.R. LAJOIE and R.E. WALLACE (1984): Modification of wave-cut and faulting-controlled landforms, *J. Geophys. Res.*, **89**, 5771-5790.

HANKS, T.C. and R.E. WALLACE (1985): Morphological analysis of the Lake Lahontan shoreline and beachfront fault scarps, Pershing County, Nevada, *Bull. Seismol. Soc. Am.*, **75**, 835-846.

HANKS, T.C. and D.P. SCHWARTZ (1987): Morphologic dating of the pre-1983 faulting event on the Lost River fault at Doublespring Pass Road, Custer County, Idaho, *Bull. Seismol. Soc. Am.*, **77**, 837-846.

HARDEN, J.W. (1982): A quantitative index of soil development from field descriptions: examples from a chronosequence in Central California, *Geoderma*, **28**, 1-28.

HARDEN, J. W. and E.M. TAYLOR (1983): A quantitative comparison of soil development in four climatic regimes, *Quat. Res.*, **20**, 342-359.

JACOBY, G.C., P.L. WILLIAMS and B.M. BUCKLEY (1992): Tree ring correlation between prehistoric landslides and abrupt tectonic events in Seattle, Washington, *Science*, **259**, 1621-1623.

KARLIN, R.E. and S.E.B. ABELLA (1992): Paleoearthquakes in the Puget Sound region recorded by sediments from Lake Washington, U.S.A., *Science*, **259**, 1617-1620.

KELLER, E.A. (1986): Investigation of active tectonics: use of surficial earth processes, in: *Studies in Geophysics, Active Tectonics*, National Academy Press, Washington D.C., pp. 136-147.

KENNEDY, G.L., K.R. LAJOIE and J.F. WEHMILLER (1982): Aminostratigraphy and faunal correlations of late Quaternary marine terraces, Pacific coast, U.S.A., *Nature*, **299**, 545-547.

LAJOIE, K.R., (1986): Coastal Tectonics, in: *Active Tectonics, Studies in Geophysics*, National Academy Press, Washington D. C., pp. 95-124.

LINDVALL, S.C., T.K. ROCKWELL and K.W. HUDNUT (1989): Evidence for prehistoric earthquakes on the Superstition Hills fault from offset geomorphic features, *Bull. Seismol. Soc. Am.*, **79**, 342-361.

MACHETTE, M.N. (1985): Calcic soils of the Southwestern United States, in: *Soils and Quaternary Geology of the Southwestern United States*, edited by D.L. WEIDE, *Geol. Soc. Am. Bull.*, **203**, 1-21.

MACHETTE, M.N., S.F. PERSONIUS, A.R. NELSON, D.P. SCHWARTZ and W.R. LUND (1991): The Wasatch fault zone, Utah - segmentation and history of Holocene earthquakes, *J. Struct. Geol.*, **13**, 137-149.

MATSUDA, G. (1977): Estimation of future destructive earthquake from active faults in Japan, *J. Phys. Earth.*, **25** suppl., 251-260.

MAYER, L. (1986): Tectonic geomorphology of escarpments and mountain fronts, in: *Studies in Geophysics, Active Tectonics*, National Academy Press, Washington D. C., pp. 125-135.

MCFADDEN, L.D. and J.C. TINSLEY (1985): Rate and depth pf pedogenic-carbonate accumulation in soils: formulation and testing of a compartment model, *Soils and Quaternary Geology of the Southwestern United States*, edited by D. L. Weide, *Geol. Soc. Am. Bull.*, **203**, 23-41.

MCGILL, S. F. and K. SIEH (1991): Surficial offset on the Central and Eastern Garlok fault associated with prehistoric earthquakes, *J. Geophys. Res.*, **96**, 21597-21621.

MEGHRAOUI, M., H. PHILIP, F. ALBAREDE and A. CISTERNAS (1988): Trench investigations through the trace of the 1980 El Asnam thrust fault: evidence for paleoseismicity, *Bull. Seismol. Soc. Am.*, **78**, 979-999.

NASH, D.B. (1980): Morphologic dating of degraded fault scarps, *J. Geol.*, **88**, 353-360.

NASH, D.B. (1986): Morphologic dating and modeling degradation of fault scarps, in: *Studies in Geophysics, Active Tectonics, National Academy Press*, Washington D. C., pp. 181-194.

NIEMI, T.M. and N.T. HALL (1992): Late Holocene slip rate and recurrence of great earthquakes on the San Andreas fault in Northern California, *Geology*, **20**, 195-198.

PANTOSTI, D., D.P. SCHWARTZ and G. VALENSISE (1993): Paleoseismology along the 1980 Irpinia earthquake fault and implications for earthquake recurrence in the Southern Apennines, *J. Geophys. Res.*, **98** (in publication).

PEARSON, G.W., J.R. PILCHER, M.G.M. BAILLIA, D.M. CORBETT and F. QUA (1986): High precision ^{14}C measurements of Irish Oaks to show the natural ^{14}C variations from A. D. 1840-5210 B. C., *Radiocarbon*, **28** (2 B), 939-942.

SCHUMM, S. A. (1986): Alluvial river response to active tectonics, in: *Studies in Geophysics, Active Tectonics*, National Academy Press, pp. 80-94.

SCHUSTER, R.L., R.L. LOGAN and P.T PRINGLE (1992): Prehistoric Rock avalanches in the Olimpic Mountains, Washington, *Science*, **259**, 1620-1621.

SCHWARTZ, D.P. (1987): Earthquakes of the Holocene, *Rev. Geophys.*, **25** (6), 1197-1202.

SCHWARTZ, D.P. (1988): Paleoseismicity of the Cordillera Blanca fault zone, Northern Peruvian Andes, *J. Geophys. Res.*, **93**, 4712-4730.

SCHWARTZ, D.P. (1990): Geologic characterization of seismic sources: moving into the 1990s, Proceedings of the: *Conference of the American Society of Civil Engineers: Earthquake Engineering and Soil Dynamics II*, June 1988, pp. 1-42.

SCHWARTZ, D.P., K.L. HANSON and F.H SWAN III (1983): Paleoseismic investigations along the Wasatch fault zone: an update, *Spec. Stud. Utah Geol. Mineral. Surv.*, **62**, 45-49.

SCHWARTZ, D.P. and K.J. COPPERSMITH (1984): Fault behavior and characteristic earthquakes: examples from the Wasatch and San Andreas fault zones, *J. Geophys. Res.*, **89**, 5681-5698.

SEGALL, P. and M. LISOWSKI (1990): Surface displacements in the 1906 San Francisco and Loma Prieta earthquakes, *Science*, **250**, 1241-1244.

SHEPPARD, P. R. and G.C. JACOBY (1989): Application of tree ring analysis to paleoseismology - 2 case studies, *Geology*, **17**, 226-229.

SIEH, K.E. (1978): Prehistoric large earthquakes produced by slip on the San Andreas Fault at Pallet Creek, California, *J. Geophys. Res.*, **83**, 3907-3939.

SIEH, K. E. (1981): A review of geological evidence for recurrence times of large earthquakes, in: *Earthquake prediction-An international review*, Am. Geophys. Union, Washington D.C., pp. 181-207.

SIEH, K.E. (1984): Lateral offsets and revised dates of large prehistoric earthquakes at Pallett Creek, Southern California, *J. Geophys. Res.*, **89**, 7641-7670.

SIEH, K.E. and R.H. JAHNS (1984): Holocene activity of

the San Andreas at Wallace Creek, California, *Geol. Soc. Am. Bull.*, **95**, 883-896.
SIEH, K.E. and P.L. WILLIAMS (1990): Behavior of the Southernmost San Andreas fault during the past 300 years, *J. Geophys. Res*, **95**, 6629-6645.
STUIVER, M., T.F. BRAZIUNAS, B. BECKER and B. KROMER (1991): Climatic, solar, oceanic, and geomagnetic influences on late-glacial and Holocene atmospheric $^{14}C/^{12}C$ change, *Quat. Res.*, **35**, 1-24.
TALWANI, P. and J. COX (1985): Paleoseismic evidence for recurrence of earthquakes near Charleston, South Carolina, *Science*, **229**, 379-381.
TSUTSUMI, H., A. OKADA, T. NAKATA and M. ANDO (1992): Near surface structure and Holocene movements on the Okamura fault, an active segment of the median tectonic line in Central Shikoku - a case study of the 1988 spring trench survey, *Mem. Geol. Soc. Jap.*, **40**, 43-127(in Japanese).
VALENSISE, G. and S. WARD (1991): Long-term uplift of the Santa Cruz coast line in response to repeated earthquakes along the San Andreas fault, *Bull. Seismol. Soc. Am.*, **81**, 1694-1704.
VALENSISE, G. and D. PANTOSTI (1992): A 125 Kyr-long geological record of seismic source repeatability: the Messina Straits (Southern Italy) and the 1908 earthquake (M_S 7½), *Terra Nova*, **4**, 472-483.
WALLACE, R.E. (1977): Profiles and age of young fault scarps, North-Central Nevada, *Bull. Geol. Soc. Am.*, **88**(9), 1267-1281.
WELDON, R.J. (1991): Active tectonic studies in the United States, 1987-1990, *Rev. Geophys.*, pp. 890-906.
WELDON, R. J. and K.E. SIEH (1985): Holocene rate of slip and tentative recurrence interval for large earthquakes on the San Andreas fault, Cajon Pass, Southern California, *Geol. Soc. Am. Bull.*, **96**, 793-812.
ZHANG, P., D.B. SLEMMONS and F. MAO (1991): Geometric pattern, rupture termination and fault segmentation of the Dixie Valley-Pleasent Valley active normal fault system, Nevada, U.S.A., *J. Struct. Geol.*, **13**, 165-176.